

# Application of Nonisothermal Cure Kinetics to the Interaction of Poly(ethylene terephthalate) with Alkyd Resin Varnish

D. S. Dias, M. S. Crespi, C. A. Ribeiro, M. Kobelnik

São Paulo State University, Universidade Estadual Paulista (UNESP), Instituto de Química, Araraquara, Brazil

Received 24 October 2007; accepted 23 August 2009

DOI 10.1002/app.31371

Published online 18 August 2010 in Wiley Online Library (wileyonlinelibrary.com).

**ABSTRACT:** Samples of varnish (V), poly(ethylene terephthalate) from recycled soft drink bottles (PET-R), and varnish/poly(ethylene terephthalate) from recycled soft drink bottles mixtures (VPET-Rs) were evaluated with differential scanning calorimetry (DSC) to verify their physicochemical properties and thermal behavior. Films from V and VPET-R were visually similar. The maximum amount of PET-R that we could add to V without significantly altering its filming properties, such adherence and color in glass sheets, was 2%. The cure process (80–203°C) was identified through the DSC curves. The kinetic parameters, activation energy ( $E$ ), and Arrhenius parameter ( $A$ ) for the

samples containing 0.5–2% PET-R were calculated with the Flynn–Wall–Ozawa isoconversional method. With greater amounts of PET-R added, there was a small change in  $E$  for the curing process. A kinetic compensation effect, represented by the equation  $\ln A = -10.5 + 0.29E$ , was observed for all of the samples. The most suitable kinetic model to describe this curing process was the autocatalytic Sestak–Berggren model, which is applied to heterogeneous systems governed by nucleation and growth. © 2010 Wiley Periodicals, Inc. *J Appl Polym Sci* 119: 1316–1321, 2011

**Key words:** poly(ethylene terephthalate); resin; kinetics

## INTRODUCTION

Industrial activity and household consumption generate an ever-growing amount of waste products that pose environmental risks and are a matter of concern for public environmental agencies. Thermosets are among the most environmentally damaging waste products because of their slow degradation. Thus, the recycling of those polymeric materials is of great interest not only to researchers and users but also to those concerned with the protection of the environment. Currently, one of the polymers found in large quantities in urban solid waste is poly(ethylene terephthalate) from recycled soft drink bottles (PET-R); it is used in the production of a variety of goods, such as fibers and films, or incorporated into other types of plastics as an additive.<sup>1</sup>

Because PET-R is a polycondensation polymer formed by ethylene glycol (EG) and terephthalic acid (t-PA), it can be used in the synthesis of coating materials where alkyd resins are used. These coating polyesters synthesized from poly(ethylene terephthalate) (PET), EG, and t-PA have similar characteristics and the structure of a polyester synthesized from

EG and phthalic anhydride. The polycondensation that takes place during the reaction causes the depolymerization of PET, EG, and t-PA, with unpredictable distributions in the polymer. The properties of films formed from PET-R, EG, and t-PA are comparable with those of conventional film coatings.<sup>2</sup> Thermogravimetry/derivative thermogravimetry (TG/DTG) curves have been used to establish the thermal decomposition reaction and kinetic parameters of alkyd resins from commercial varnishes (V's).<sup>3,4</sup>

The aim of this study was to evaluate the maximum amount of PET from the reutilization soft drink bottles that could be added to commercial alkyd resin V through differential scanning calorimetry (DSC) curves of the curing reaction of the film.

### Kinetic aspects

The mathematical description of the data from a single step solid-state decomposition is usually defined in terms of a kinetic triplet, with the activation energy ( $E$ ), Arrhenius parameter ( $A$ ), and a mathematical expression of the kinetic model as a function of the fractional conversion [ $f(\alpha)$ ], which can be related to the experimental data as follows:<sup>5</sup>

$$\frac{d\alpha}{dt} = A \exp\left(-\frac{E}{RT}\right) f(\alpha) \quad (1)$$

where  $T$  is temperature in Kelvin,  $t$  is time in minute, and  $\alpha$  is the fractional conversion. For dynamic data obtained at a constant heating rate ( $\beta = dT/dt$ ),

Correspondence to: D. S. Dias (diosanto@iq.unesp.br).  
Contract grant sponsor: Conselho Nacional de Desenvolvimento Científico e Tecnológico (CNPq) (Brazil).

this new term is inserted into eq. (1), which can be simplified as

$$\frac{d\alpha}{dT} = \frac{A}{\beta} \exp\left(-\frac{E}{RT}\right) f(\alpha) \quad (2)$$

$E$  from dynamic data can be obtained from the Flynn–Wall–Ozawa isoconversional method<sup>6–8</sup> with Doyle’s approximation of  $p(x)$ ,  $p(x)$  is defined by equation  $\int_x^\infty \frac{e^{-x}}{x^2} dx$ , temperature integral or integral of Arrhenius<sup>9</sup> which involves the measurement of temperature corresponding to fixed values of  $p(x)$  obtained from experiments at different  $\beta$ ’s and the plotting of  $\ln \beta$  versus  $1/T$ :

$$\ln \beta = \left[ \frac{AE}{Rg(\alpha)} \right] - 5.331 - 1.052 \frac{E}{RT} \quad (3)$$

where  $R$  is the universal gas constant ( $8.31432 \text{ K}^{-1} \text{ J}^{-1}$ ) and  $g(\alpha)$  is the integral of  $d\alpha/f(\alpha)$  from 0 to  $\alpha$ .

This method allows one to obtain the apparent  $E = E(\alpha)$  independently of the kinetic model, where  $E(\sigma)$  is the activation energy for specific conversion degree ( $\sigma$ ). One evaluates the pre-exponential factor by taking into account that the reaction is a first-order one and can be defined as<sup>10</sup>

$$A = \frac{\beta E}{RT_m^2} \exp\left(\frac{E}{RT_m}\right) \quad (4)$$

### Kinetic model determination

The rate of the kinetic process ( $d\alpha/dt$ ) through DSC curves is based on the following relation:

$$\frac{d\alpha}{dt} = \frac{\phi}{\Delta Hc} \quad (5)$$

where  $\phi$  is the heat flow normalized per sample mass,  $\Delta H$  is the enthalpy change associated with this process, and  $c$  is crystallization.

The rate of the kinetic process can be expressed by

$$\frac{d\alpha}{dt} = K(T)f(\alpha) \quad (6)$$

where

$$K(T) = A \exp\left(-\frac{E}{RT}\right) \quad (7)$$

The shape of a dynamic DSC curve at a specific  $\beta$  with any kind of model considered can be written as

$$\phi = \Delta HA \exp\left(-\frac{E}{RT}\right) f(\alpha) \quad (8)$$

The test to find the kinetic model proposed by Malek<sup>11–14</sup> is based on this equation and the normalized  $y(\alpha)$  and  $z(\alpha)$  functions, which under nonisothermal conditions, are given by

$$y(\alpha) = \phi \exp\left(\frac{E}{RT}\right) = B_n f(\alpha) \quad (9)$$

where  $B_n$  is a constant equal to  $\Delta HA$  and the shape of the  $y(\alpha)$  function is formally identical to the kinetic model  $f(\alpha)$ , in which the maximum value is  $\alpha_y^*$ :<sup>10,13,15</sup>

$$z(\alpha) = \phi T \pi\left(\frac{E}{RT}\right) = \Delta H \beta f(\alpha) g(\alpha) \quad (10)$$

where  $\pi(E/RT)$  is an approximation of the integral temperature,<sup>16</sup> which in case of the  $z(\alpha)$  function,<sup>17</sup> can be obtained accurately by consideration of the approximation  $\pi \approx RT/E$ . Then

$$z(\alpha) = \phi T^2 = C_n f(\alpha) g(\alpha) \quad (11)$$

where  $C_n$  is a constant equal to  $\Delta H \beta E/R$  and the  $\alpha$  at the maximum of the  $z(\alpha)$  ( $\alpha_y^*$ ) is characteristic of any model.<sup>10,13</sup>

### EXPERIMENTAL

Postconsumer soft drink bottles with PET were washed, dried at room temperature, cut into pieces of approximately  $2 \text{ mm}^2$ , and solubilized with phenol/tetrachloromethane (1 : 1) at  $80^\circ\text{C}$ . Trichloromethane was used as the solution’s stabilizing agent.

The commercial V studied was constituted of modified alkyd resin, vegetal oil, aromatic and aliphatic hydrocarbons, and tensoactive and drying organometallic compound agents. The V was solubilized with the same method applied to the PET-R solution to prevent the precipitation of PET-R in the mixture.

After the solutions had been separately heated to  $60^\circ\text{C}$ , the PET-R solution was added drop by drop to the V solution under vigorous stirring. The mass relationships of the PET-R to V solutions are presented in Table I.

The varnish/poly(ethylene terephthalate) from recycled soft drink bottles mixtures (VPET-Rs) were then spread in film form on slides and wood and dried at room temperature to verify that their visual appearance was effectively similar. The samples were collected after 48 h to analyze their physico-chemical behavior through DSC curves.

DSC recording was done with a DSC 2910 module from TA Instruments (New Castle, DE) in a dynamic atmosphere of nitrogen (50 mL/min) covered with a  $10\text{-}\mu\text{L}$  aluminum crucible with a sample mass of

**TABLE I**  
**PET-R and V Mass Relationships for Samples 1-5**

	Sample				
	1	2	3	4	5
V (g)	10.0128	10.0046	10.0000	10.0053	10.0000
PET-R (g)	0.2003	0.1500	0.1006	0.0801	0.0503

around 2 mg, with the aluminum crucible as the reference material and  $\beta$ 's of 10, 15, and 20°C/min from 40 to 300°C. The  $E$  and  $\log A$  kinetic parameters were calculated with DSC ASTMK software version 4.08 from TA Instruments.

## RESULTS AND DISCUSSION

The DSC curve given by the second heating of the PET-R [Fig. 1(a)] presented three characteristic events comparable with data reported in the literature,<sup>2</sup> which were (1) a vitreous transition temperature at about 85°C, (2) a crystallization temperature at 154°C, and (3) a melting temperature at 250°C.

The DSC curve for V [Fig. 1(b)] showed no significant thermal event in the temperature interval 0–300°C, and the DSC curve for VPET-R sample 1 [Fig. 1(c)] presented an exothermic peak (80–203°C) for the first heating caused by the cure reaction of the sample, whereas in the second heating curve [Fig. 1(d)] that peak disappeared, which indicated a complete reaction; that is, the material had already been completely cured.

To establish the kinetic model for the curing reaction, we obtained the kinetic parameters,  $E$ , and the pre-exponential factor,  $\log A$ , from the DSC curve of sample 1 (VPET-R sample 1) at three different  $\beta$ 's (10, 15, and 20°C/min; Fig. 2) within the temperature range used in this study, applying the Flynn–Wall–Ozawa isoconversional method.<sup>6,18,19</sup>

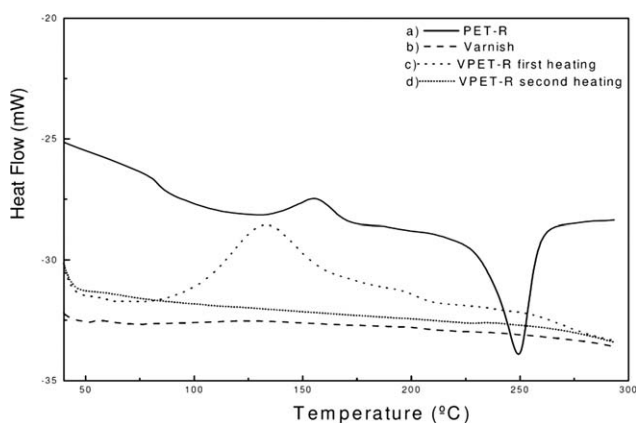


**Figure 1** DSC curves for the PET-R, V, VPET-R first-heating, and VPET-R second-heating samples under a nitrogen atmosphere with a  $\beta$  of 10°C/min.

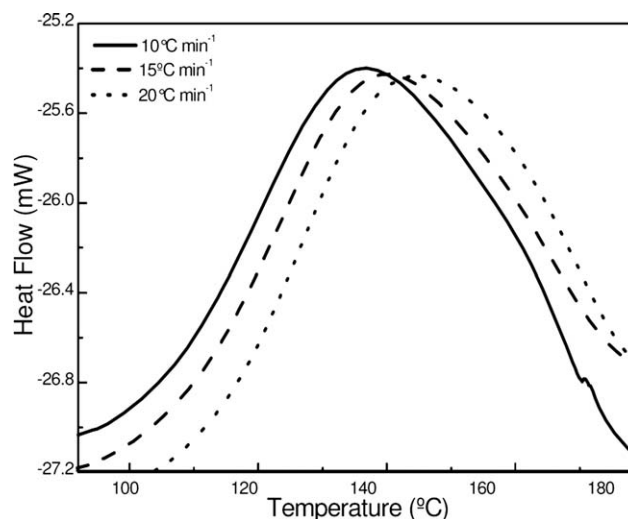


**Figure 2** DSC curves to the VPET-R 1 under a nitrogen atmosphere ( $\beta = 10, 15,$  and  $20^\circ\text{C}$ ).

For each fixed fractional conversion  $\alpha$  and corresponding temperature,  $E$  could be calculated from the slope of the plot of  $\ln(\beta)$  versus  $1000/T$  [eq. (3); Fig. 3].

The obtained results had to be within the limit to be the Doyle approximation to  $p(x)$ , in which  $20 \leq E/RT \leq 50$ . Thus, the average values, at a 95% confidence level, found for  $E$  and  $\log A$  for DSC were  $72.1 \pm 9.1$ ,  $116.5 \pm 12.4$ ,  $96.4 \pm 3.3$ ,  $73.0 \pm 4.3$ , and  $96.4 \pm 2.2$  kJ/mol.

Figure 4 shows  $\alpha$ , independent of the apparent values of  $E$ . The nearly constant  $E$  values were obtained within a range of  $0.05 \leq \alpha \leq 0.95$ , with mean values of 72.1, 116.5, 96.4, 73.0, and 96.4 kJ/mol for VPET-R samples 1, 2, 3, 4, and 5, respectively. The  $E$  values being similar at different  $\alpha$ 's was a prerequisite for the application of the general eq. (4). The results in Figure 4 indicate that this reaction could be treated within the restricted range of  $0.1 \leq \alpha \leq 0.8$ .<sup>20</sup>

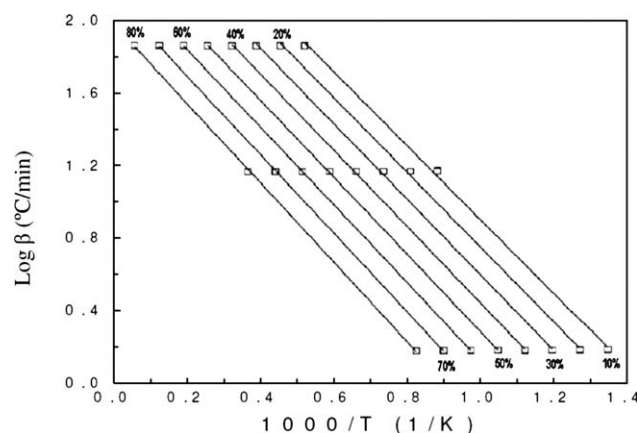


**Figure 3** Plot of  $\log \beta$  against  $1/T$  at various  $\alpha$  values to obtain  $E$  (Flynn–Wall–Ozawa method).

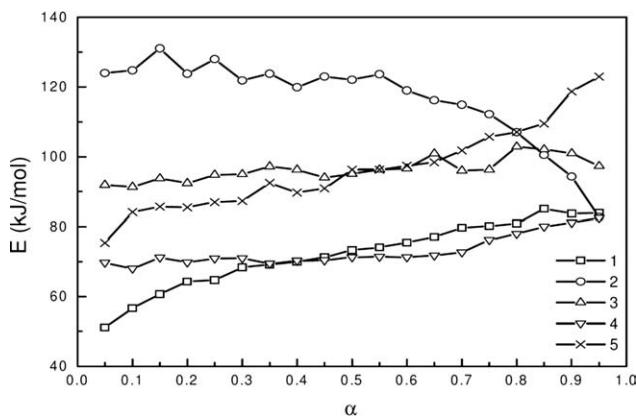


**Figure 4** Values of  $E$  at various  $\alpha$ 's calculated by the Flynn–Wall–Ozawa method for VPET-R samples 1–5.

The observed linearity of several  $\alpha$ 's indicated that the proposed kinetic model could be used to evaluate the curing reaction of VPET-R.

Once the  $E$  values were defined, it was possible to establish the best kinetic model to describe that set of measurements obtained via the DSC curves.

To this end, the  $y(\alpha)$  and  $z(\alpha)$  functions were used, as they could be easily obtained by transformations of the experimental data expressed by eqs. (9) and (11), respectively.

The  $y(\alpha)$  function is proportional to the  $f(\alpha)$  function, which must be invariable in relation to the experimental parameters, such as sample mass and  $\beta$  (nonisothermal conditions) or temperature (isothermal conditions). Thus, we obtained the form of the  $f(\alpha)$  function by plotting the normalized  $y(\alpha)$  between 0 and 1, which is the characteristic of a specific kinetic model. The  $\alpha$  values between 0.05 and 0.95 and the respective temperatures were obtained from the nonisothermal DSC curves (10, 15, and

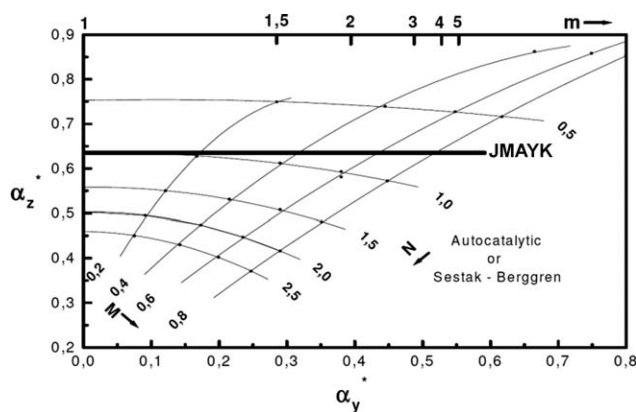


**Figure 5**  $\alpha_y^* - \alpha_z^*$  plot for the two-parameter autocatalytic model. The fine lines show the influence of the kinetic exponents  $m$  and  $n$ . JMAYK, Johnson, Mehl, Avrami, Yerofeev and Kolmogorov;  $M$  and  $N$ , kinetic exponent of Sestak-Berggren equation  $f(\alpha) = \alpha^M (1 - \alpha)^N$  also known as auto-catalytic model;  $m$  is the kinetic exponent to JMAYK model.

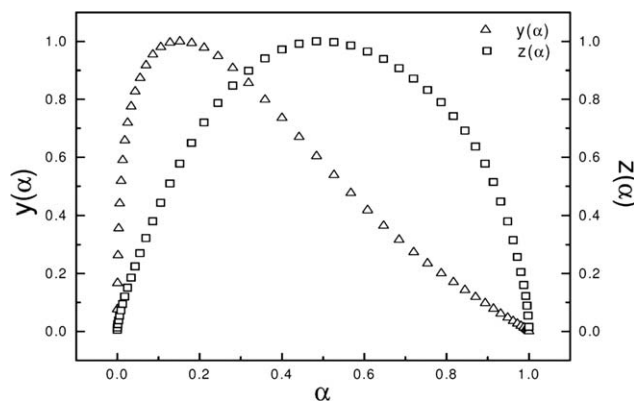


**Figure 6**  $y(\alpha)$  and  $z(\alpha)$  functions calculated from the DSC data for VPET-R sample 1.

20°C/min), whereas  $\phi$  was obtained by subtraction of the base line values from those of the cure process curves.

A more reliable test of the applicability of the kinetic model was based on the properties of the  $y(\alpha)$  and  $z(\alpha)$  function. These maxima of these functions are  $\alpha_y^*$  and  $\alpha_z^*$ , respectively. If the maximum falls into the  $0.61 \leq \alpha_z^* \leq 0.65$  range, the experimental data probably correspond to the Johnson, Mehl, and Avrami (JMA) model. If the maximum is shifted to lower values of  $\alpha$  ( $\alpha_z^* < 0.6$ ), the condition of validity of the JMA model is not fulfilled.<sup>13</sup>

If the  $y(\alpha)$  function has a maximum and  $\alpha_z^* \ll 0.632$ , the Sestak-Berggren (SB) model can be used. The SB model can be described by means of an empirical two-parameter model:

$$f(\alpha) = \alpha^m(1 - \alpha)^n \quad (12)$$

where  $m$  and  $n$  are parameter kinetic exponents.<sup>21</sup> The maximum  $\alpha_y^*$  of the  $y(\alpha)$  function can be expressed as  $\alpha_y^* = (m/m + n)$  and  $\alpha_z^* > \alpha_y^*$ .<sup>22</sup> Figure 5 shows the  $\alpha_y^* - \alpha_z^*$  diagram calculated for a constant value of parameters  $m$  and  $n$  of the autocatalytic model or SB model.

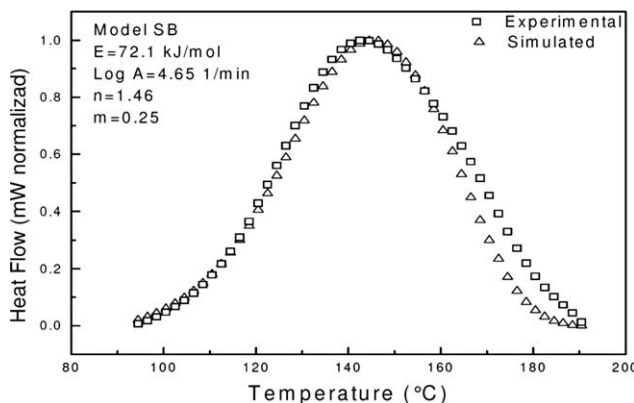


**Figure 7** Experimental and simulated DSC curves at 10°C/min for VPET-R sample 1.

**TABLE II**  
Average  $E$ ,  $\log A$ , and  $r^2$  Values;  $y(\alpha)$  and  $z(\alpha)$  Maximum Functions; Kinetic Exponents Calculated from the SB Model; and Values of the Kinetic Parameters for Samples 1–5

Sample	$E$ (kJ/mol)	$\log A$ (1/min)	$r^2$	$\alpha_y^*$	$\alpha_z^*$	$n$	$m$
1	$72.1 \pm 9.1$	$4.65 \pm 0.93$	0.9924	0.15	0.48	1.46	0.25
2	$116.5 \pm 12.4$	$10.35 \pm 1.95$	0.9943	0.01	0.51	1.84	0.03
3	$96.4 \pm 3.3$	$7.78 \pm 0.26$	0.9940	0.08	0.48	0.74	0.15
4	$73.0 \pm 4.3$	$4.80 \pm 0.32$	0.9985	0.17	0.55	1.27	0.26
5	$96.4 \pm 2.2$	$7.75 \pm 1.13$	0.9957	0.10	0.50	1.50	0.17

The DSC curves obtained with eqs. (9) and (11) showed that the  $y(\alpha)$  function yielded a maximum when  $\alpha_y^* = 0.15$  and  $z(\alpha), \alpha_z^* = 0.48$  for the VPET-R sample 1 (Fig. 6). Applying the values obtained in diagram (Fig. 5), we verified that the SB model was the most appropriate to represent the curing process for these samples.<sup>11</sup>

The  $n$  kinetic exponent can be obtained from the angular coefficient of  $\ln[(d\alpha/dt) \exp(E/RT)]$  versus  $\ln[\alpha^p(1 - \alpha)]$  in the range of  $0.2 < \alpha < 0.8$ . For sample 1,  $n = 1.46$ , and, therefore,  $m = 0.25$ , with the relation of  $m = pn$ , where  $p = \alpha_y^*/(1 - \alpha_y^*)$ .

Figure 7 presents the DSC curves for the simulated and experimental data, which shows that the SB model described the curing mechanism for sample 1 and that this mechanism could also be applied to the other samples.

Table II presents the  $E$ ,  $\log A$ , correlation coefficient ( $r^2$ ),  $\alpha_y^*$ ,  $\alpha_z^*$ ,  $n$ , and  $m$  values for the curing reactions.

To samples with amounts of PET-R in the V upper 2% there was a beginning of precipitation in the reaction medium, with white dots showing across the length of the surface of the film.

### Kinetic compensation effect

The kinetic compensation effect was first developed in catalysis studies to account for the fact that differ-

ent treatments of a catalyst resulted in a change in the calculated  $E$  but with no corresponding change in the reaction velocity with the rate of the reaction remaining constant. The dependences of  $E$  and the pre-exponential factor on the degree of conversion generally reflects the existence of a compensation effect, which corresponds to the validity of the following relation:<sup>23</sup> in accordance with eq. (12):

$$\ln A = a + bE \quad (13)$$

where  $a$  and  $b$  are constants referred to as compensation parameters.

This effect has been observed in many types of reactions. The kinetic parameters ( $A$  and  $E$ ) vary with the experimental conditions even if the mechanism does not change.

The thermal reaction of a polymer is a complex solid-gas reaction. For the cure reaction of VPET-R sample 1,  $\ln A$  was plotted against  $E$ , as shown in Figure 8. Such a relationship indicates that  $\ln A = -10.5 + 0.29E$ .

In this study, we verified that the amount of mass of PET-R in V increased up to a limit of 2%, and the curing reaction mechanism in all of the samples was the same as was observed from the straight-sloped line between  $\ln A$  and  $E$ .<sup>24–28</sup>

### CONCLUSIONS

The experimental data from the curing process under nonisothermal conditions allowed the kinetic triplet [ $E$ ,  $\log A$ , and  $f(\alpha)$ ] to be calculated. The kinetic procedures applied in this study were consistent for obtaining the kinetic parameters and a mathematical kinetic model function. On the basis of the best fit between the normalized simulated data with the SB kinetic model function and the experimental data, it was evident that the curing process presents an initial step explained by an induction characteristic that is autocatalytic behavior, which are applied to heterogeneous systems.

Thus, the kinetic behavior of the curing of VPET-R samples 1–5 was correlated with the compensation phenomena. The linear relationship between  $\ln A$  and  $E$  revealed compensation due to various factors.

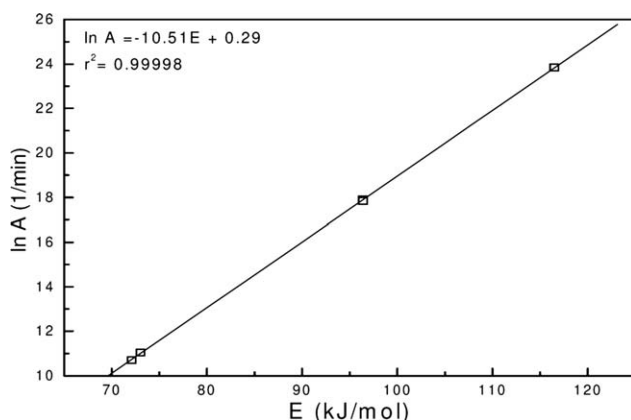


**Figure 8** Arrhenius plots of  $\ln A$  versus  $E$  for the cure reactions of VPET-R sample 1.

Little change was found in the  $E$  values from 72.1 to 96.4 kJ/mol, whereas the physical chemical properties (appearance) of the film obtained, such as adherence, color, and flexibility, were similar to those of commercial alkyd V, which makes the process proposed here, technologically viable.

## References

1. Mano, E. B.; Mendes, L. C. *Introdução a Polímeros*; Edgard Blucher: São Paulo, Brazil, 1999.
2. Kawamura, C.; Ito, K.; Nishida, R.; Yoshihara, I.; Numa, N. *Prog Org Coat* 2002, 45, 185.
3. Amaral, G. C. A.; Crespi, M. S.; Ribeiro, C. A.; Hikosaka, M. Y.; Guinese, L. S.; Santos, A. F. J. *Therm Anal Cal* 2005, 79, 375.
4. Dias, D. S.; Crespi, M. S.; Ribeiro, C. A.; Fernandes, J. L. S.; Cerqueira, H. M. G. *J Therm Anal Calorim* 2008, 91, 409.
5. Brown, M. E.; Dolimore, D.; Galwey, A. K. *Reactions in the Solid State: Comprehensive Chemical Kinetics*; Elsevier: Amsterdam, 1980.
6. Flynn, J. H.; Wall, L. A. *J Res Natl Bur Stand A* 1966, 70, 487.
7. Flynn, J. H.; Wall, L. A. *Polym Lett* 1966, 4, 323.
8. Dahiya, J. B.; Kumar, K.; Muller-Hagedorn, M.; Bockhorn, H. *Polym Int* 2008, 57, 722.
9. Doyle, C. D. *J Appl Polym Sci* 1962, 6, 639.
10. Kissinger, H. E. *Anal Chem* 1957, 29, 1702.
11. Málek, J.; Šesták, J.; Rouquerol, F.; Rouquerol, J.; Criado, J. M.; Ortega, A. *J Therm Anal* 1992, 38, 71.
12. Malek, J. *J Therm Anal Calorim* 1999, 56, 763.
13. Malek, J. *Thermochim Acta* 2000, 355, 239.
14. Málek, J.; Mitisuhash, T.; Criado, J. M. *J Mater Res* 2001, 16, 1862.
15. Silva, A. R.; Crespi, M. S.; Ribeiro, C. A.; Oliveira, S. C.; Silva, M. R. S. *J Therm Anal Calorim* 2004, 75, 401.
16. Sestak, J. *Thermophysical Properties of Solids: Their Measurements and Theoretical Analysis*; Elsevier: Amsterdam, 1984.
17. Malék, J. *Thermochim Acta* 1995, 267, 61.
18. Ozawa, T. *Bull Chem Soc Jpn* 1965, 38, 1881.
19. Ozawa, T. *J Therm Anal* 1970, 2, 301.
20. Koga, N. *Thermochim Acta* 1995, 258, 145.
21. Malek, J. J. *Thermochim Acta* 1989, 138, 337.
22. Sestak, J. *Science of the Heat and Thermophysical Studies: A Generalized Approach to Thermal Analysis*; Elsevier: Amsterdam, 2005.
23. Budrugaec, P.; Homentcovschi, D.; Segal, E. *J Therm Anal Calorim* 2001, 63, 457.
24. MacCallun, R.; Munro, M. V. *Thermochim Acta* 1992, 203, 457.
25. Gupta, C.; Viswanath, S. G. J. *Thermal Anal* 1996, 47, 1081.
26. Prasad, T. P.; Kanungo, S. B.; Ray, H. S. *Thermochim Acta* 1992, 203, 503.
27. Brown, M. E.; Galwey, A. K. *Thermochim Acta* 2002, 387, 173.
28. Galwey, A. K. *Thermochim Acta* 2004, 413, 139.